Sorptive removal of dissolved organic matter in biologically-treated effluent by functionalized biochar and carbon nanotubes: importance of sorbent functionality

Mohammad Boshir Ahmed, Md. Abu Hasan Johir, Chinu Khourshed, John L. Zhou, Huu Hao Ngo, Duc Long Nghiem, Mohammad Moni, Lying Sun

PII: S0960-8524(18)31149-0
DOI: https://doi.org/10.1016/j.biortech.2018.08.046
Reference: BITE 20329

To appear in: *Bioresource Technology*

Received Date: 13 July 2018
Revised Date: 13 August 2018
Accepted Date: 13 August 2018

Please cite this article as: Boshir Ahmed, M., Abu Hasan Johir, Md., Khourshed, C., Zhou, J.L., Hao Ngo, H., Long Nghiem, D., Moni, M., Sun, L., Sorptive removal of dissolved organic matter in biologically-treated effluent by functionalized biochar and carbon nanotubes: importance of sorbent functionality, *Bioresource Technology* (2018), doi: https://doi.org/10.1016/j.biortech.2018.08.046

Sorptive removal of dissolved organic matter in biologically-treated effluent by functionalized biochar and carbon nanotubes: importance of sorbent functionality

Mohammad Boshir Ahmed[a], Md. Abu Hasan Johir[a], Chinu Khourshed[b], John L. Zhou[a*], Huu Hao Ngo[a], Duc Long Nghiem[a], Mohammad Moni[c], Lying Sun[d]

[a]School of Civil and Environmental Engineering, University of Technology Sydney, 15 Broadway, NSW 2007, Australia

[b]ICP Laboratory, SSEAU, Mark Wainwright Analytical Centre, University of New South Wales, NSW 2052, Australia

[C]Sydney Medical School, The University of Sydney, NSW 2006, Australia

[d]Key Laboratory of Water Cycle and Related Land Surface Processes, Institute of Geographical Sciences and Natural Resources Research, Chinese Academy of Sciences, Beijing 100101, China

[*]Corresponding author

Prof John L. Zhou

School of Civil and Environmental Engineering

University of Technology Sydney

15 Broadway, NSW 2007, Australia

Email: junliang.zhou@uts.edu.au

Abstract

The sorptive removal of dissolved organic matter (DOM) in biologically-treated effluent was studied by using multi-walled carbon nanotube (MWCNT), carboxylic functionalised MWCNT (MWCNT-COOH), hydroxyl functionalized MWCNT (MWCNT-OH) and functionalized biochar (fBC). DOM was dominated by hydrophilic fraction (79.6%) with a significantly lower hydrophobic fraction (20.4%). The sorption of hydrophobic DOM was not significantly affected by the sorbent functionality (~10.4% variation) and sorption capacity followed the order of MWCNT > MWCNT-COOH > MWCNT-OH > fBC. In comparison, the sorption of hydrophilic fraction of DOM changed significantly (~37.35% variation) with the change of sorbent functionality with adsorption capacity decreasing as MWCNT-OH > MWCNT-COOH > MWCNT > fBC. Furthermore, the affinity of adsorbents toward a hydrophilic compound (dinitrobenzene), a hydrophobic compound (pyrene) and humic acid was also evaluated to validate the proposed mechanisms. The results provided important insights on the type of sorbents which are most effective to remove different DOM fractions.

Keywords: DOM fractions; Functionality; Hydrophobic fraction; Hydrophilic fraction; MWCNT

1. Introduction

Dissolved organic matter (DOM) with a wide variety of chemical compositions and molecular sizes is ubiquitous in different types of water (Fu et al., 2017; Shimabuku et al., 2017). DOM is originated from plant litter, soil, humus, microbial biomass (with aquagenic and pedogenic sources) degradation, root exudates, and living or decayed vegetation (Conte et al., 2011; Fu et al., 2017). DOM has an average concentration of 0.5 to 10.0 mg L^{-1} in natural water (Genz et al., 2008). DOM anthropogenically impacted water and wastewater and plays an essential role in environmental and engineered aquatic systems (Fu et al., 2017; Shimabuku et al., 2017). For example, DOM can serve as an energy source for bacteria, attenuate light, and influence the fate and transport of contaminants. Although DOM is regarded as non-toxic, however, many problems may arise with the naturally coloured groundwater. These leads direct concern to taste and odour problems of water (Cornelissen et al., 2008; Genz et al., 2008). DOM is also responsible for membrane fouling; poor oxidation of iron and manganese; and biological instability of drinking water in distribution systems (re-growth) (Amy and Cho 1999; Lee et al., 2018; Li et al., 2016; Peldszus et al., 2011; Sánchez-Martín et al., 2010; Van der Kooij 2003; Xing et al., 2008; Yang et al., 2017). In addition, the presence of DOM is responsible for the formation of disinfection by-products (DBP) such as trihalomethanes and haloacetic acids (Fu et al., 2017; Genz et al., 2008; Golea et al., 2017). Furthermore, residual natural organic matter can promote bacterial regrowth and pipe corrosion in the drinking water distribution system (Song et al., 2009). The content of NOM (especially for the hydrophobic fraction) in surface waters is increasing rapidly due to change in natural environment (Levchuk et al., 2017). The water-derived DOM contains a low amount of phenolic and aromatic compounds, whereas soil-derived DOM contains higher lignin content and aromatic fraction (Fu et al., 2017). Based on hydrophobicity, the components in DOM can be divided into hydrophobic and hydrophilic fractions.

To remove DOM, most commonly used methods are coagulation and flocculation followed by sedimentation/flotation and granular media filtration. However, coagulation mainly removes hydrophobic fraction of DOM rather than the hydrophilic fraction (Sharp et al., 2006). Unfortunately, the residual DOM after coagulation generally have significant DBP formation potential and need additional treatments to remove the residual DOM (Sharp et al., 2006). It is recommended by the US EPA for the control of DBP precursors (Kim and Kang, 2008). Furthermore, Biological system can promote the microbial growth and biofilm formation in the biofilters, subsequently enhancing the removal of NOM. Biopolymers can be well removed by biofiltration system, whereas low removal was found for humic acid fractions such as humic substances, building blocks, low MW neutrals and low MW acids (Chen et al., 2016). Granular activated carbon (GAC) has been employed to remove DOM as well as taste and odour through direct competition column bed and mentioned that pore blockage occurred due to fouling by DOM (Summers et al., 2013). Carbon nanotubes (CNTs), with their high surface area, hydrophobicity, porosity, and rapid sorption kinetics, have been explored for the interactions with DOM (Engel and Chefetz, 2015; 2016; Peng et al., 2017a). Therefore, materials characteristics, DOM molecular structure and composition, and the solution chemistry (e.g. pH, water temperature, and ionic strength) are prime factors affecting sorption of DOM (Hyung and Kim, 2008; Li et al., 2014; Wang et al., 2013). However, it is more difficult to explain how DOM characteristics influence its adsorption behaviour as DOM is composed of a mixture of heterogeneous compounds possessing highly different physical and chemical properties. Several studies have shown that DOM molecular size can determine its adsorption behaviour (Newcombe et al., 1997a; Newcombe et al., 1997b; Velten et al., 2011). In addition, DOM aromaticity and polarity can be important characteristics (Zietzschmann et al., 2015), yet it remains unclear which characteristics govern DOM adsorption.

It is generally expected that sorption of hydrophobic and hydrophilic organic compounds is affected by the increase or decrease of the sorbent hydrophobicity or hydrophilicity (Peng et al., 2017b; Teixidó et al., 2011). However, the comprehensive studies in the literature examining the adsorption of DOM fractions, based on sorbent functionality, by carbonaceous materials (CMs) are rare. Therefore, the main objective is to apply several CMs having unique functionalities (such as functionalized biochar (fBC), MWCNT, MWCNT-COOH and MWCNT-OH) to investigate the effect of functional groups for the adsorption of hydrophilic and hydrophobic fractions of DOM from membrane bioreactor (MBR) effluent. This will provide detailed knowledge on how the sorbents' surface functional groups influence the removal of different DOM fractions and what type of adsorbent is most effective for DOM removal.

2. Materials and methods

2.1. *Chemicals and sorbents*

All chemicals including 1,3-dinitrobenzene (DNB), pyrene (PYE), standard solutions (for Na, K, Mg, Fe, Pb, Mn, Ni, Ca, and Cu), KCl, Na_2CO_3 and $NaHCO_3$ were of analytical grade and purchased from Sigma Aldrich, Australia. Three types of CMs namely, multiwalled carbon nanotube (MWCNT, specific surface area > 90 $m^2 g^{-1}$), carboxylic group functionalized MWCNT (MWCNT-COOH, specific surface area > 117 $m^2 g^{-1}$), hydroxyl group functionalized MWCNT (MWCNT-OH, specific surface area >117 $m^2 g^{-1}$); and functionalized biochar (fBC, surface area 2.18 $m^2 g^{-1}$) having distinct physical structures and chemical compositions, were used as sorbents. All MWCNTs have an outer and inner diameter of 8-15 and 3-5 nm, respectively and was > 99.9% pure. All MWCNTs were purchased from Chengdu Organic Chemistry Co., Chinese Academy of Sciences, China. Biochar was first prepared from *Eucalyptus globulus* wood via pyrolysis at 380 ^{0}C under continuous nitrogen supply at 1 psi. Then produced biochar was washed with milli-Q water

for several times and adjusted the solution pH to 7.0 and finally dried at furnace at 105 ^{o}C. fBC was prepared from biochar (produced at 380 ^{o}C) using phosphoric acid as activating and functionalized agent at 600 ^{0}C. A detailed preparation procedure of fBC is reported in our previous studies (Ahmed et al., 2017a; 2017b; 2017c; 2018).

2.2. *Characteristics of MBR effluent*

Municipal effluent was collected from a membrane bioreactor at Central Park, Sydney, Australia. After collection, the MBR effluent was filtered through 1.2 μm glass fiber filter and physicochemical properties such as pH, turbidity, UV_{254}, total organic carbon (TOC), chemical oxygen demand (COD), conductivity, alkalinity, dissolved oxygen, inorganic ions, and metal ions were measured as listed in **Table 1**.

2.3. Sorption experiments

The sorption of DOM and its fractions in MBR effluent was conducted in 250 mL conical fluxes at 25 ^{o}C in duplicate on an orbital shaker over 48 h at 120 rpm using different CMs. Dosages of fBC, MWCNT, MWCNT-COOH and MWCNT-OH were selected based on removal capacity of all DOM fractions. Pristine biochar was also used for DOM removal but found with low removal efficacy of 7.2%. Therefore, pristine biochar was not utilized for further experiments. Initial and diluted MBR effluent samples were used for DOM isotherm study. Dilution of MBR effluent was carried out with MQ water with the same pH as MBR effluent. The control experiments without sorbent were also conducted. Initial and final pH and conductivity were measured.

The sorption of DNB, PYE and humic acid was performed individually. The initial concentrations of DNB, PYE and humic acid were 5.0 mg L^{-1}, 1.0 mg L^{-1} and 13.67 mg L^{-1}, respectively. These concentration were chosen based on sorbent types and removal efficacy. The adsorbent dosage used was 50-70 mg L^{-1}. Control experiments were also performed under the same condition. After the sorption experiments, the supernatants were filtered

through 0.45-μm (for DNB and PYE) and 1.2-μm (for DOM and humic acid) syringe filters before analysis.

2.4. *Chemical analysis of MBR effluent*

The concentration and the fractionation of DOM were carried out using liquid chromatography-organic carbon detector (LC-OCD). LC-OCD result also provides detail information on the hydrophilic and hydrophobic fractions of DOM together with quantitative and qualitative results regarding molecular size distribution of organics present in water and wastewater. As required, samples were pre-filtered using 0.45 μm cellulose nitrate membrane filters (Fisher Scientific, USA). UV_{254} absorbance analysis of treated and untreated MBR effluent at 254 nm was measured at room temperature using Shimadzu UV-visible spectroscopy instrument (UV-1700). Metal cation contents in raw and treated MBR effluent were analysed using inductive coupled plasma mass spectroscopy (ICP-MS 7900, Agilent Technologies, Japan). Inorganic anions were analysed for phosphate, chloride, nitrate, nitrite and sulphate using a Metrohm ion chromatography (IC) (model 790 Personal IC). The IC was equipped with an autosampler and conductivity cell detector. Na_2CO_3 (3.2 mmol L^{-1}) and $NaHCO_3$ (1.0 mmol L^{-1}) were used as a mobile phase with 0.7 mL min^{-1} flow rate. The results provide a more robust understanding of the adsorption behaviour of DOM fractions on MWCNTs and fBC for MBR effluent treatment.

DNB concentration (as a representative hydrophilic compound) was analysed by a high performance liquid chromatography (HPLC) equipment with an auto-sampler and a UV detector. A reverse-phase Zorbax Bonus RP C_{18} column (5.0 μm, 2.1 ×1.50 mm) was used throughout for detection and quantification of HOCs. The volume of injection was 100 μL. Mobile phase A was composed of acetonitrile and formic acid (99.9: 0.1) while mobile phase B was composed of Milli-Q water and formic acid (99.9: 0.1). The elution used 40% of A and 60% of B at a flow rate of 0.4 mL min^{-1} and maintained 6 min. The UV wavelength for the whole method was selected at 285 nm and switched to 240 nm from 4.00 min to 5.00 min for

DNB detection. PYE concentration was measured using a UV-Vis spectroscopy with a specific wavelength of 240 nm. The DOM concentration of humic acid solution was measured by total organic carbon (TOC) analyser and using a UV-Vis spectroscopy with a specific wavelength of 254 nm. Any samples that could not be analysed immediately were stored at 4 ^{0}C.

2.5. *Physical characterizations of sorbents*

The physicochemical characteristics of fBC and MWCNTs were extensively examined using Fourier transform infrared spectroscopy (FTIR, Miracle-10: Shimadzu), scanning electron microscopy (SEM, Zeiss Evo-SEM system), X-ray diffraction (XRD) analysis, and zeta potential measurement. SEM was used to determine the morphological properties of CMs. XRD analysis of the samples was carried out using a Bruker D8 Discover diffractometer using Cu Kα radiation, in the scattering angle 2θ range 20°–60°. FTIR was used to determine surface functional groups. The iso-electric values (zeta potential) of fBC and MWCNTs (dosage, 40-70 mg L^{-1}) were measured by suspending into 1 mM KCl solution in the pH range of 1.45–10.20 separately using a Zetasizer Nano instrument (Nano ZS Zen3600, Malvern, UK). Samples were pre-equilibrated for ~48 h. Measurements in triplicate (average 30 scans with settling time of 5 s) were made to minimise undesirable biases, and the average value with standard deviation was used for data analyses.

2.6. *Modelling of sorption data*

Adsorption capacity, i.e. solid phase sorption (q_s, μg g^{-1}) of DOM was calculated using following equations.

$$Adsorption\ capacity, q_s = \frac{C_0 - C_e}{m} \times V \quad (1)$$

where C_0 and C_e are the initial and equilibrium concentration of DOM (mg L^{-1}), m is the mas of sorbent used (g) and V is the volume of solution (L).

Isotherm models employed to fit the adsorption isotherms are as follows:

$$\text{Langmuir model: } q_s = \frac{q_{max} K_L C_e}{1 + K_L C_e} \quad (2)$$

where q_{max} is the maximum adsorption capacity (mg g^{-1}) and K_L is the Langmuir fitting parameter (L mg^{-1}). Parameters were estimated by nonlinear regression weighted by the dependent variable.

$$\text{The Freundlich model: } q_s = K_f C_e^{\,n} \quad (3)$$

where q_s is the solid-phase sorbed capacity (mg g^{-1}) of DOM fractions, n is a dimensionless number related to surface heterogeneity, and K_f is the Freundlich affinity coefficient (mg^{1-n} L^n g^{-1}). C_e represents the aqueous-phase concentration of solute (mg L^{-1}) at 25 ^{0}C. All model equations were fitted by origin-pro, with model parameters being obtained with a standard coefficient of determination (r^2) and adjusted coefficient of determination (r_{adj}^2).

3. Results and discussion

3.1. *Characteristics of sorbents*

All three MWCNTs have randomly distributed surface and grooves. MWCNTs appear to form bundles or aggregates driven by van der Waals forces due to their high hydrophobicity. These surface, groove, interstitial and inner areas on MWCNTs offer many sites for adsorption of organic chemicals (Wang et al., 2017).

XRD spectra of fBC consists of amorphous structure, and broad peak appeared at 25-30°. On the other hand, it is evident that the general trends of all three MWCNTs plots, which can be ascribed to their crystalline arrangements, are very similar. Thus, it can be concluded that functionalization process of graphitised MWCNTs did not affect the graphitic structure of MWCNTs significantly. Obviously; these plots show the expectable characteristic of a MWCNT structure. The C(002) peak around 2θ = 26.2° is flatten due to the limited number of layers and tube curvature represent a typical phase of CNT or graphite. As shown in these patterns, the intensity of C(002) in MWCNT is much lower than MWCNT-OH and MWCNT-COOH. This can be attributed to the higher packing density in MWCNT-COOH and MWCNT-OH and defects caused by functionalization. The peaks appearing at 42.3°, 44.5°,

54.5 °, 59.8 ° and 77.8° refer to the crystalline plane diffraction peaks. In all cases, higher peak intensity was observed for MWCNT-COOH followed by MWCNT-OH and MWCNT.

The FTIR spectra of fBC, MWCNT, MWCNT-OH and MWCNT- COOH possess a peak at 1589.7-1598.52 cm^{-1} corresponds to C=C double bond of nanotubes. The peak at 3770-3780 is attributed to hydroxyl (–OH) stretching vibration. Peaks at 1720 represent the C=O bonds. The simultaneous presence of these two peaks characterises the appearance of the carboxyl group on the surface of MWCNT. Two peaks at ~2030 and ~2100 indicate the presence of CH group in MWCNTs. On the other hand, fBC consist of different functional groups especially graphitic carbon (~57%), phenolic or alcoholic (C-O-, ~13.5%), carbonyl or quinone (C=O, ~4%), carboxylic or ester (COO-, ~3%), π-π* transition (~1%), quaternary nitrogen (~1%), and polyphosphates and/or phosphates (C-O-PO_3, ~1%) (Ahmed et al., 2018). Structural analysis of carbon network showed that fBC was composed of mesopore (2-50 nm) and macrospore (> 50 nm) structure (Ahmed et al., 2018). The point of iso-electric charge for fBC was pH 2.2 (Ahmed et al., 2018). The point of iso-electric charge for MWCNT, MWCNT-COOH and MWCNT-OH was found to be 4.47, 4.36 and 5.14 (**Figure 1**).

3.2. *MBR effluent properties*

The pH, conductivity and turbidity of MBR effluent were 7.94 (±0.06), 7.95 (μS cm^{-1}) and 0.42 (NTU), respectively. The concentrations of DOM and inorganic carbon content in MBR effluent were 8.63 mg L^{-1} and 48.15 mg L^{-1}, respectively. The UV_{254} adsorption value and chemical oxygen demand of the MBR effluent were 0.269 cm^{-1}, and 28.3 mg L^{-1}, respectively. Characteristics of MBR effluent is shown in **Tables 1** and **2**. UV_{254} and SUVA values (from LC-OCD) also reduced significantly depending on the type of sorbents which indicated the removal of DOM fractionations. MWCNT-COOH and MWCNT-OH have higher removal efficacy of SUVA and UV_{254} values of MBR effluent than fBC and MWCNT (**Table 2**).

The higher amount of metal ions such as sodium ion (198.96 mg L^{-1}), potassium ion (31.42 mg L^{-1}), calcium ion (12.90 mg L^{-1}) and magnesium ion (4.72 mg L^{-1}) were also found in MBR effluent, and they might have negative effect on DOM sorption. Further, MBR effluent also contained higher concentration of nitrate ion (35.97 mg L^{-1}), sulphate ion (33.02 mg L^{-1}) and chloride ion (2.56 mg L^{-1}). After adsorption experiments with CMs, the concentration of anions did not decrease, which can be explained by the zeta potential values of fBC and CMs. For example, fBC, MWCNT, MWCNT-COOH and MWCNT-OH zeta potential values were 2.2, 5.12, 4.47 and 4.78, respectively (**Figure 1**). The surface of CMs at pH 7.94 were negative. Therefore, electrostatic repulsion between negative CMs surfaces and negative anions should be the main reason for insignificant sorption of all anions.

3.3. *Adsorption affinity of DOM and its fractions*

Data on DOM adsorption have been fitted to two different isotherm models (**Table 3**). The Freundlich sorption isotherm model provided slightly better fit with the experimental data than the Langmuir isotherm model for all sorbents, as indicated by the coefficient of determination values (r^2 and adjusted r^2). The maximum adsorption capacity of DOM (40.68 mg g^{-1}) was observed for hydroxyl functionalized MWCNT followed by MWCNT (39.30 mg g^{-1}), MWCNT-COOH (36.23 mg g^{-1}), and fBC (7.81 mg g^{-1}). The Freundlich adsorption coefficient value of fBC, MWCNT, MWCNT-COOH and MWCNT-OH were found to be 1.32, 4.11, 5.32 and 6.50 ($mg^{1-n} L^n g^{-1}$), respectively. The Freundlich parameter *n* values of DOM ranged from 0.58 to 0.71 (from fBC to MWCNT). Thus, DOM sorption onto fBC and MWCNTs were non-linear indicating that favorable for multilayer adsorption and non-heterogeneous energy distribution of fBC and MWCNTs. Therefore, DOM sorption onto fBC and MWCNTs mostly followed the monolayer cover according to Langmuir postulates as well as multilayer coverage according to the Freundlich postulates. However, the Langmuir adsorption isotherm sorption capacity among different MWCNTs varies by 10%, and the Freundlich isotherm coefficient value of MWCNTs varies more significantly (up to 58%).

This information primarily implies that the ionizable functional groups of DOM (i.e. carboxylic and phenolic group) may govern adsorption of DOM based on the type of functionality of the sorbent. From the above result it is found that sorption of DOM is greatly affected by CMs material type and surface functionality has great influence toward adsorption of fractionations of DOM.

From the DOM fractionation of MBR effluent, it is found that the percentage of hydrophobic and hydrophilic organic fraction is 20.4% (1.76 mg L^{-1}) and 79.6% (6.87 mg L^{-1}), respectively. In hydrophilic organics, the amount of biopolymers (MW >> 20,000), humic substances (HS, MW ~1000), building blocks (MW 300-500), LMW neutrals (MW < 350) and LMW acids (MW < 350) were 58. 50, 0.74, 1.14 and 0 mg L^{-1}, respectively.

3.4. *Hydrophobic DOM removal by sorbents*

The physical properties of MWCNTs play an important role in the adsorption of DOM. Selected MWCNT is hydrophobic (graphitic) and are primarily made up of SP^2 hybridisation and carbon atoms densely packed in a hexagonal honeycomb crystal lattice (Wang et al., 2017). Hence, graphitic properties of MWCNT and SP^2 structure suggest that hydrophobic and π-π may occur between the graphitic surface and DOM hydrophobic fractions. On the other hand, the introduction of O-containing functional groups (e.g. –COOH & -OH) into MWCNTs (e.g. MWCNT-COOH & MWCNT-OH) disrupted the π-electronic system of the graphitic layer of MWCNTs as a result of $SP^2 \rightarrow SP^3$ rehybridization, leading to breaks up the delocalized π-band structure of graphitic structure and act as a scattering center in the graphene lattice also associated with their adsorption capacity (Wang et al., 2017).

The hydrophobic fraction of DOM consists of high amount of aromatic carbon, phenolic structures and conjugated double bond compounds (Fu et al., 2017). This aromatic carbon conjugated double bonds and phenolic structures in DOM may interact with sorbent graphitic sites i.e. carbon-carbon double bonds by hydrophobic effect, π-π interactions and also by π-hydrogen bond formation. **Figure 2** shows the hydrophobic DOM removal by different CMs.

For fBC sorbent, the results show that fBC adsorbs slightly higher amount of hydrophobic fraction than hydrophilic fraction of DOM. This can be explained by its hydrophobicity and hydrophilicity of fBC. fBC contains 57% graphitic carbon which might be responsible for hydrophobic part of DOM adsorption through interaction via hydrophobic effect and π-π interactions with π-electron systems of an aromatic carbon, phenolic structure and conjugated double bonds π-systems of DOM. On the other hand, MWCNT has slightly higher sorption capacity of hydrophobic fraction than MWCNT-COOH and MWCNT-OH. This indicates that presence of different atoms in MWCNT change the properties of graphitic carbon so-called rehybridization (Wang et al., 2017). The adsorption of hydrophobic fraction of DOM can be explained by hydrophobic effect and π-π interactions among graphitic carbon of MWCNTs and aromatic carbon, phenolic ring and conjugated double bonds of DOM. The main reason for the slight decrease of sorption capacity of MWCNT-COOH and MWCNT-OH was due to the presence of oxygenated functional groups in MWCNT (Wang et al., 2017; Wang et al., 2013). However, one might assume that there was no significance difference on sorption performance of hydrophobic fraction of MBR effluent among MWCNTs. This can be explained by the degree of surface functionality in MWCNT. For example, MWCNT-COOH contains~1.28% (wt) of –COOH functional group and MWCNT-OH contains ~1.85% (wt) of hydroxyl functional group. This data clearly indicate the role of surface functionality of MWCNTs. Therefore, due to the surface functionality of MWCNT-COOH and MWCNT-OH, sorption of hydrophobic fraction of DOM was reduced to few extend (10.4%) as hydrophobic interaction sites were occupied by other functional groups, thereby reducing the sorption capacity of hydrophobic DOM fraction.

The effect of hydrophilicity and hydrophobicity of sorbent is further examined by the adsorption of a hydrophobic organic compound such as pyrene (PYE) onto fBC, MWCNT, MWCNT-COOH and MWCNT-OH. The result is shown in **Figure 2**. PYE is a π-electron donor by virtue of its π-electron donor ability. The previous study showed that PYE was able

to form a π-π complex between the π-electrons of benzene rings of PYE and active graphene layers on activated carbon due to electron-donor-acceptor (EDA) mechanism (Xiao et al., 2015). Our study shows that adsorption of PYE was maximum for MWCNT followed by MWCNT-COOH, MWCNT-OH and fBC (**Figure 2**). This can be explained by the graphene layer of MWCNT which is hydrophobic moiety and PYE is also hydrophobic properties. Therefore, one possible explanation for maximum sorption of PYE by MWCNT can be hydrophobic interaction due to their hydrophobicity (PYE and MWCNT hydrophobic). π-π interactions between electrons reach benzene ring of PYE which could act as electron-donor site and negative surface of MWCNT (zeta potential is negative) which could act as the electron-acceptor site might also responsible for higher sorption of hydrophobic fraction of DOM. Thereby, apart from hydrophobic interaction, π-π electron donor-acceptor (EDA) interactions played a vital role in adsorption of PYE onto MWCNT. However, this tendency was significantly reduced when introduced hydrophilic character onto MWCNT, i.e. functionalization of MWCNT. Lower adsorption of PYE by functionalized MWCNTs was expected due to the introduction of oxygen atoms in MWCNT which reduce the hydrophobicity of MWCNT. Thence, the lower adsorption capacity of hydrophobic compound (PYE) onto relatively lower hydrophobic MWCNTs (i.e. MWCNT-COOH and MWCNT-OH) indicated the insignificant role of other interactions such as hydrogen bond formations.

Hence, sorption of hydrophobic fraction of DOM mainly occured due to hydrophobic effects (between DOM and sorbent) and π-π EDA interactions. Slight reduction of graphitic carbon percentage in MWCNT (i.e. reduced hydrophobicity of MWCNT) led to decrease in sorption capacity. Therefore, hydrophobic fraction adsorption onto CMs can be significantly changed with the change of surface functionality of CMs. However, the relative lower percentage of surface functionalization of MWCNT would only cause insignificant adsorption difference of hydrophobic DOM.

3.5. *Hydrophilic DOM removal by sorbents*

Hydrophilic DOM fraction (79.6%) usually has more aliphatic carbon and nitrogenous compounds, such as carbohydrates, sugars and amino acids (Fu et al., 2017). The hydrophilic fraction is generally humic substances (57.2%, MW ~1000), comprised of humic acids (HA), fulvic acids (FA) and humin, which make up more than 50% of the total organic carbon in water (Cornelissen et al., 2008). Apart from humic substances, other hydrophilic fractions of MBR effluent in DOM consisted of biopolymers (0.7%), building blocks (8.6%), and low molecular weight neutrals (12.7%).

The removal of hydrophilic fraction of DOM by different CMs was of opposite trend to that of hydrophobic fraction of DOM. Overall, among CMs, MWCNT-OH showed the highest removal of hydrophilic fractions of DOM followed by MWCNT-COOH, MWCNT and fBC (**Figure 3)**. Functionalized MWCNT (e.g. –OH functionalized) showed 37.35% higher adsorption capacity of hydrophilic DOM fraction over graphitized MWCNT. This primarily represents that the functionalization of MWCNT increase the adsorption of hydrophilic DOM. The presence of the oxygen-containing groups (more hydrophilic in nature) on the surface of MWCNT caused a reduction of their adsorption capacities of hydrophobic compounds, but the adsorption of hydrophilic organic contaminants may increase or decrease depending on each other's polarity (Ateia et al., 2017). The oxygen content in the functionalized MWCNTs, used in this study, were in the range of 1.28-1.85% (wt % of graphitized MWCNT). The higher removal of hydrophilic fraction by MWCNT-OH over graphitized MWCNT can be explained by the presence of more oxygen content (~1.85 wt. %) in MWCNT. Therefore, along with hydrophobic interactions non-hydrophobic interactions such as π-π interactions, hydrogen bond formation, and electrostatic interactions between functional groups of functionalized MWCNTs and with hydrophilic groups of DOM (e.g., COOH and –OH) were also played a vital role for adsorption of hydrophilic DOM fraction. In addition, the BET results showed that the MWCNTs had different surface areas

(90-117 $m^2 g^{-1}$) and thus pore filling mechanism might also be a responsible mechanism. Therefore, O-containing functional groups can alter the adsorption of MWCNTs by reducing the hydrophobicity of functionalized MWCNTs and weakening the hydrophobic effects.

The effect of hydrophilicity and hydrophobicity is further examined by the adsorption of a model hydrophilic organic compound such as 1,3-dinitrobenzene (DNB) onto fBC, MWCNT, MWCNT-COOH and MWCNT-OH (**Figure 3)**. DNB is a strong π-electron acceptor by viture of its π-electron acceptability (Chen et al., 2008). On the other hand, increasing pH facilities deprotonation of the acidic functional groups such as –COOH and –OH of MWCNTs, which can promote the π-electron donor ability of the graphene surface of MWCNTs compared to MWCNT. Therefore, EDA interactions between DNB and deprotonated graphene surface of functionalized MWCNTs is responsible for higher adsorption of DNB than MWCNT (Chen et al., 2008). However, the maximum adsorption capacity of DNB was observed for fBC. This was due to the presence of a lower degree of graphitic carbon (57%) and higher degree oxygen-containing surface functional groups. Therefore, adsorption of the hydrophilic organic compound on the graphene surfaces of fBC and MWCNTs was mainly due to account for the stronger non-hydrophobic adsorptive interactions. Such interactions might include hydrogen bond formation and electrostatic interactions.

Hence, the oxygen content of MWCNTs was responsible for the adsorption behaviour indicating the role of functional groups for sorption of hydrophilic moiety of DOM (Wang et al., 2017). Overall, surface functionality has significant influence in the sorption of hydrophilic DOM in MBR effluent.

3.5.1. Humic substance removal by sorption

The number-average molecular weight (M_w, 734) and number-average molecular number (M_n, 378) of humic substances changed with sorbent type. Among different sorbents, MWCNT caused the largest reduction of M_n from 378 to 309, more than other adsorbents such as fBC

(from 378 to 377), MWCNT-COOH (from 378 to 331) and MWCNT-OH (from 378 to 330). The ratio of M_w to M_n *(i.e.* M_w/M_n) also changed simultaneously.

Figure 4 shows the removal of humic substances (2nd column) by CMs, demonstrating that functionalized MWCNTs had higher sorption capacity of humic substances than graphitic MWCNT. MWCNT-OH showed highest sorbed capacity (~8.00 mg g^{-1}) followed by MWCNT-COOH (~6.40 mg g^{-1}), MWCNT (~6.10 mg g^{-1}) and fBC (1.15 mg g^{-1}). Higher sorption of humic substances by functionalized MWCNTs primarily indicated the role of surface functionalization over non-functionalized graphitic MWCNT. Therefore, the role of non-hydrophobic interactions such as hydrogen bond formations and π-π interactions along with hydrophobic interactions could also contribute to the overall sorption of humic substances. Humic substances such as humic acid, fulvic acid and humins have different functional groups such as –COOH; -OH; C=O; -O-; -COO-. Protonated functional groups (i.e. –COOH and -OH) could get deprotonated at used pH (i.e. 7.94). The initial pH of MBR effluent was 7.94, at which point those functional groups could deprotonate and the deprotonated surface of humic substances could act either as π-electron acceptor site and π-electron donor site. For example, -OH groups in CMs could act as π-electron donor site and –COOH groups in CMs could act as π-electron acceptor site in the used condition (Ahmed et al., 2017c). On the other hand, the MWCNT surface could act as π-electron donor site while functionalized MWCNTs deprotonated at this pH and could act as the π-acceptor site. Therefore, opposite pair of EDA interactions were played a vital role in adsorption of humic substances. Other non-hydrophobic interactions such as hydrogen bond between oxygenated functional groups of adsorbent and adsorbate also played a role in overall adsorption.

Figure 5a shows the removal of humic acid (HA synthetic, measured in terms of DOM) by CMs. Functionalized MWCNTs obtained maximum adsorption of humic acid. Higher adsorption of humic acid by MWCNTs than fBC was due to the mainly higher surface area of MWCNTs. However, maximum sorption capacity of MWCNT-OH and MWCNT-

COOH should be due to EDA interactions and hydrogen bonds formation by the oxygenated functional groups. The absence of oxygenated functional groups in MWCNT did not facilitate the formation of hydrogen bond, hence leading to lower adsorption capacity of humic acid by MWCNT.

Figure 5b shows the removal of dissolved organic nitrogen (DON) present in humic acid. It was found that functionalized MWCNTs had higher sorption of DON than MWCNT. The presence of (hetero)aromatic amine cations can act as π acceptors in forming π^{+}–π electron donor-acceptor (EDA) interactions with the π electron-rich, the polyaromatic surface of CMs (Xiao and Pignatello, 2015). Therefore, due to EDA interactions and hydrogen bonding capability of functionalized MWCNTs they can adsorb higher amount of DON.

3.5.2. Removal of LMW neutral compound by sorbents

MWCNT showed highest sorption of LMW neutral (2.16 mg g^{-1}) followed by MWCNT-OH (1.93 mg g^{-1}), MWCNT (1.77 mg g^{-1}) and fBC (0.61 mg g^{-1}) (**Figure 4**). Slightly higher sorption of LMW neutral by MWCNT also indicated that the adsorption was similar to the adsorption of the hydrophobic compound. Therefore, the hydrophobicity and the hydrophilicity of surface functional groups in both adsorbent and adsorbate play a vital role in their sorption behaviour.

3.5.3. Removal of biopolymer and building block by sorbents

The removal of biopolymer and building blockers also followed the same trend as observed for humic substances removal, i.e. MWCNT-OH > MWCNT-COOH > MWCNT. However, sorption of biopolymers was found minimum compared to humic substances, LMW neutrals and building blockers. This might be due to their large molecular structure and their adsorption onto CMs requires greater potential and molecular arrangement toward the specific direction of CMs and on its functional groups. Moreover, CMs and their functional groups were unable to interact with biopolymer molecules therefore showing lower adsorption.

Among fractionations of hydrophilic DOM showed the general tread of humic substances > building blockers > LMW neutral substances > biopolymers.

3.6. *Simultaneous removal of metal ions*

Table 4 shows the removal of metal ions by different CMs. It can be observed that all the CMs could remove different metal ions to some extent. This is desirable as MBR effluent had an initial pH of 7.94 and the iso-electric values of fBC and all MWCNTs were below 5.14. It is common that oppositely charged ions (i.e. negative surface of CMs and the positive surface of heavy metal ions) can interact together due to electrostatic interaction. Hence, the electrostatic interaction was the main cause for competitive adsorption of metal ions.

4. Conclusions

The maximum DOM sorption capacity was observed for functionalized sorbent MWCNT-OH followed by MWCNT-COOH, MWCNT and fBC. Sorbent hydrophobicity and hydrophilicity greatly affected DOM adsorption. MWCNT adsorbed slightly higher amount (10.4%) of hydrophobic DOM fraction than functionalized MWCNTs, whereas functionalized MWCNTs adsorbed higher amount (~37.35%) of hydrophilic DOM fraction. These findings were confirmed by separate sorption experiments using model hydrophobic, hydrophilic and humic acid compounds. Different hydrophobic and non-hydrophobic interaction such as EDA interactions, hydrogen-bond formation and electrostatic interactions were key adsorption mechanisms. The results provide guidance for selecting the correct sorbents for the removal of specific DOM fractions.

Conflict of Interests

The authors declare no competing financial interest.

Appendix: Supporting Information

Supplementary data associated with this article can be found, in the online version.

Acknowledgements

We acknowledge a HDR Post Thesis Publication Scholarship at the Faculty of Engineering and Information Technology from University of Technology Sydney, Sydney, Australia.

References

1. Ahmed, M.B., Zhou, J.L., Ngo, H.H., Guo, W., Johir, M.A., Sornalingam, K., Belhaj, D., Kallel, M., 2017a. Nano-Fe^0 immobilized onto functionalized biochar gaining excellent stability during sorption and reduction of chloramphenicol via transforming to reusable magnetic composite. Chem. Eng. J. 322, 571-581.
2. Ahmed, M.B., Zhou, J.L., Ngo, H.H., Guo, W., Johir, M.A.H., Sornalingam, K., 2017b. Single and competitive sorption properties and mechanism of functionalized biochar for removing sulfonamide antibiotics from water. Chem. Eng. J. 311, 348-358.
3. Ahmed, M.B., Zhou, J.L., Ngo, H.H., Guo, W., Johir, M.A.H., Sornalingam, K., Rahman, M.S., 2017c. Chloramphenicol interaction with functionalized biochar in water: sorptive mechanism, molecular imprinting effect and repeatable application. Sci. Total Environ. 609, 885-895.
4. Ahmed, M.B., Zhou, J.L., Ngo, H.H., Johir, M.A.H., Sornalingam, K., 2018. Sorptive removal of phenolic endocrine disruptors by functionalized biochar: Competitive interaction mechanism, removal efficacy and application in wastewater. Chem. Eng. J. 335, 801-811.
5. Amy, G., Cho, J., 1999. Interactions between natural organic matter (NOM) and membranes: rejection and fouling. Water Sci. Technol. 40(9), 131-139.

6. Ateia, M., Apul, O.G., Shimizu, Y., Muflihah, A., Yoshimura, C., Karanfil, T., 2017. Elucidating adsorptive fractions of natural organic matter on carbon nanotubes. Environ. Sci. Technol. 51(12), 7101-7110.
7. Chen, F., Peldszus, S., Elhadidy, A.M., Legge, R.L., Van Dyke, M.I., Huck, P.M., 2016. Kinetics of natural organic matter (NOM) removal during drinking water biofiltration using different NOM characterization approaches. Water Res. 104, 361-370.
8. Chen, J., Chen, W., Zhu, D., 2008. Adsorption of nonionic aromatic compounds to single-walled carbon nanotubes: effects of aqueous solution chemistry. Environ. Sci. Technol. 42(19), 7225-7230.
9. Conte, P., Abbate, C., Baglieri, A., Nègre, M., De Pasquale, C., Alonzo, G., Gennari, M., 2011. Adsorption of dissolved organic matter on clay minerals as assessed by infra-red, CPMAS ^{13}C NMR spectroscopy low field T_1 NMR relaxometry. Org. Geochem. 42(8), 972-977.
10. Cornelissen, E., Moreau, N., Siegers, W., Abrahamse, A., Rietveld, L., Grefte, A., Dignum, M., Amy, G., Wessels, L., 2008. Selection of anionic exchange resins for removal of natural organic matter (NOM) fractions. Water Res. 42(1-2), 413-423.
11. Engel, M., Chefetz, B., 2015. Adsorptive fractionation of dissolved organic matter (DOM) by carbon nanotubes. Environ. Pollut. 197, 287-294.
12. Engel, M., Chefetz, B., 2016. Adsorption and desorption of dissolved organic matter by carbon nanotubes: Effects of solution chemistry. Environ. Pollut. 213, 90-98.
13. Fu, J., Lee, W.N., Coleman, C., Meyer, M., Carter, J., Nowack, K., Huang, C.H., 2017. Pilot investigation of two-stage biofiltration for removal of natural organic matter in drinking water treatment. Chemosphere 166, 311-322.

14. Genz, A., Baumgarten, B., Goernitz, M., Jekel, M., 2008. NOM removal by adsorption onto granular ferric hydroxide: equilibrium, kinetics, filter regeneration studies. Water Res. 42(1-2), 238-248.

15. Ghernaout, D., Naceur, M., 2011. Ferrate (VI): In situ generation water treatment–A review. Desalin. Water Treat. 30(1-3), 319-332.

16. Golea, D., Upton, A., Jarvis, P., Moore, G., Sutherl, S., Parsons, S. Judd, S., 2017. THM HAA formation from NOM in raw and treated surface waters. Water Res. 112, 226-235.

17. Hyung, H., Kim, J.H., 2008. Natural organic matter (NOM) adsorption to multi-walled carbon nanotubes: effect of NOM characteristics and water quality parameters. Environ. Sci. Technol. 42(12), 4416-4421.

18. Kim, J. Kang, B., 2008. DBPs removal in GAC filter-adsorber. Water Res. 42(1-2), 145-152.

19. Lee, D. J., Cheng, Y. L., Wong, R. J., Wang, X. D., 2018. Adsorption removal of natural organic matters in waters using biochar. Bioresour. Technol. 260, 413-416.

20. Levchuk, I., Márquez, J.J.R., Sillanpää, M., 2018. Removal of natural organic matter (NOM) from water by ion exchange–A review. Chemosphere 192, 90-104.

21. Li, T., Lin, D., Li, L., Wang, Z., Wu, F., 2014. The kinetic and thermodynamic sorption and stabilization of multiwalled carbon nanotubes in natural organic matter surrogate solutions: the effect of surrogate molecular weight. Environ. Pollut. 186, 43-49.

22. Li, W.T., Jin, J., Li, Q., Wu, C.F., Lu, H., Zhou, Q., Li, A.M., 2016. Developing LED UV fluorescence sensors for online monitoring DOM and predicting DBPs formation potential during water treatment. Water Res. 93, 1-9.

23. Newcombe, G., Drikas, M., Assemi, S., Beckett, R., 1997a. Influence of characterised natural organic material on activated carbon adsorption: I. Characterisation of concentrated reservoir water. Water Res. 31(5), 965-972.

24. Newcombe, G., Drikas, M., Hayes, R., 1997b. Influence of characterised natural organic material on activated carbon adsorption: II. Effect on pore volume distribution and adsorption of 2-methylisoborneol. Water Res. 31(5), 1065-1073.

25. Peldszus, S., Hallé, C., Peiris, R.H., Hamouda, M., Jin, X., Legge, R.L., Budman, H., Moresoli, C., Huck, P.M., 2011. Reversible and irreversible low-pressure membrane foulants in drinking water treatment: Identification by principal component analysis of fluorescence EEM and mitigation by biofiltration pretreatment. Water Res. 45(16), 5161-5170.

26. Peng, M., Li, H., Li, D., Du, E., Li, Z., 2017a. Characterization of DOM adsorption of CNTs by using excitation–emission matrix fluorescence spectroscopy and multiway analysis. Environ. Technol. 38(11), 1351-1361.

27. Peng, H., Zhang, D., Pan, B., Peng, J., 2017b. Contribution of hydrophobic effect to the sorption of phenanthrene, 9-phenanthrol and 9, 10-phenanthrenequinone on carbon nanotubes. Chemosphere 168, 739-747.

28. Teixidó, M., Pignatello, J. J., Beltrán, J. L., Granados, M., & Peccia, J., 2011. Speciation of the ionizable antibiotic sulfamethazine on black carbon (biochar). Environ. Sci. Technol. 45(23), 10020-10027.

29. Sánchez-Martín, J., Ghebremichael, K., Beltrán-Heredia, J., 2010. Comparison of single-step and two-step purified coagulants from Moringa oleifera seed for turbidity and DOC removal. Bioresour. Technol. 101(15), 6259-6261.

30. Sharp, E., Jarvis, P., Parsons, S., Jefferson, B., 2006. Impact of fractional character on the coagulation of NOM. Colloid. Surf. A: Physicochem. Eng. Aspects. 286(1-3), 104-111.

31. Shimabuku, K.K., Kennedy, A.M., Mulhern, R.E., Summers, R.S., 2017. Evaluating activated carbon adsorption of dissolved organic matter and micropollutants using fluorescence spectroscopy. Environ. Sci. Technol. 51(5), 2676-2684.

32. Song, H.L., Nakano, K., Taniguchi, T., Nomura, M., Nishimura, O., 2009. Estrogen removal from treated municipal effluent in small-scale constructed wetland with different depth. Bioresour. Technol. 100(12), 2945-2951.

33. Summers, R.S., Kim, S.M., Shimabuku, K., Chae, S.H., Corwin, C.J., 2013. Granular activated carbon adsorption of MIB in the presence of dissolved organic matter. Water Res. 47(10), 3507-3513.

34. Van der Kooij, D., 2003. Biodegradable compounds biofilm formation in water treatment and distribution. Water Resources and Water Supply in the 21st Century, Hokkaido University Press, Sapporo.

35. Velten, S., Knappe, D.R., Traber, J., Kaiser, H.P., Von Gunten, U., Boller, M., Meylan, S., 2011. Characterization of natural organic matter adsorption in granular activated carbon adsorbers. Water Res. 45(13), 3951-3959.

36. Wang, F., Ma, S., Si, Y., Dong, L., Wang, X., Yao, J., Chen, H., Yi, Z., Yao, W., Xing, B., 2017. Interaction mechanisms of antibiotic sulfamethoxazole with various graphene-based materials and multiwall carbon nanotubes and the effect of humic acid in water. Carbon 114, 671-678.

37. Wang, F., Yao, J., Chen, H., Yi, Z., Xing, B., 2013. Sorption of humic acid to functionalized multi-walled carbon nanotubes. Environ. Pollut. 180, 1-6.

38. Xiao, F., Pignatello, J.J., 2015. π^{+}–π Interactions between (Hetero) aromatic amine cations and the graphitic surfaces of pyrogenic carbonaceous materials. Environ. Sci. Technol. 49(2), 906-914.

39. Xiao, X., Liu, D., Yan, Y., Wu, Z., Wu, Z., Cravotto, G., 2015. Preparation of activated carbon from Xinjiang region coal by microwave activation and its

application in naphthalene, phenanthrene, and pyrene adsorption. J. Taiwan Institute Chem. Eng. 53, 160-167.

40. Xing, W., Ngo, H. H., Kim, S. H., Guo, W. S., Hagare, P., 2008. Adsorption and bioadsorption of granular activated carbon (GAC) for dissolved organic carbon (DOC) removal in wastewater. Bioresour. Technol. 99(18), 8674-8678.

41. Yang, W., He, C., Wang, X., Zhang, Y., Cheng, Z., Dai, B., Zhang, L., 2017. Disolved organic matter (DOM) removal from bio-treated coking wastewater using a new polymeric adsorbent modified with dimethylamino groups. Bioresour. Technol. 241, 82-87.

42. Zietzschmann, F., Mitchell, R.L., Jekel, M., 2015. Impacts of ozonation on the competition between organic micro-pollutants and effluent organic matter in powdered activated carbon adsorption. Water Res. 84, 153-160.

List of Figures

Figure 1

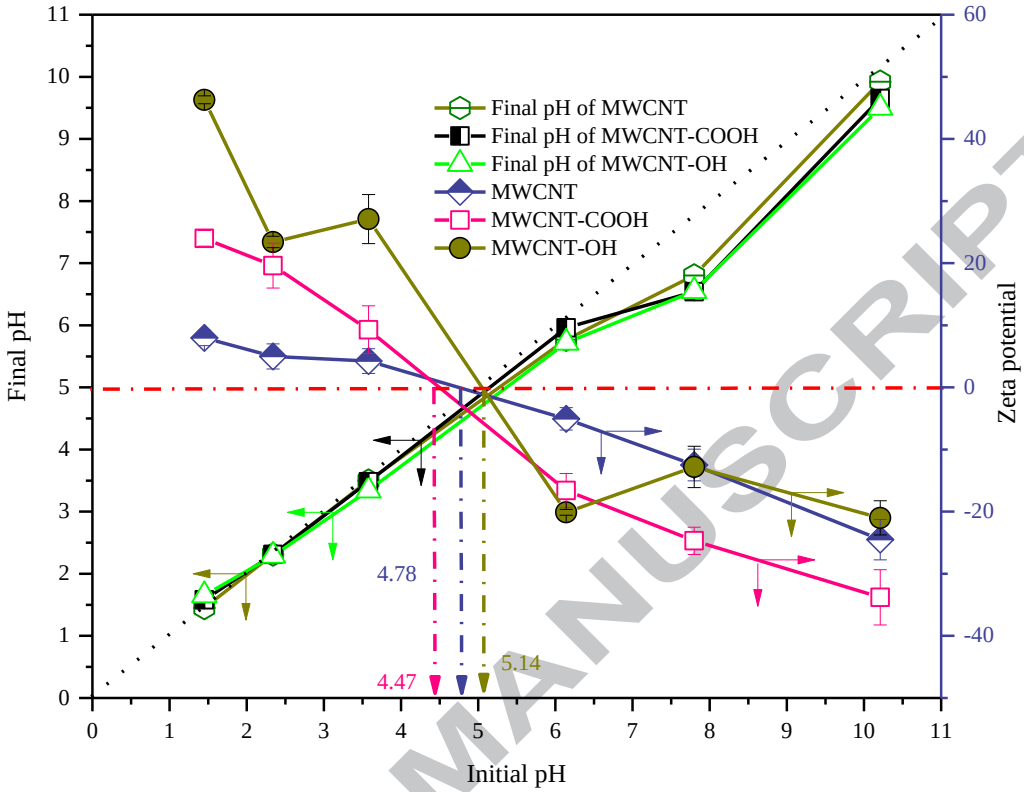

Figure 2

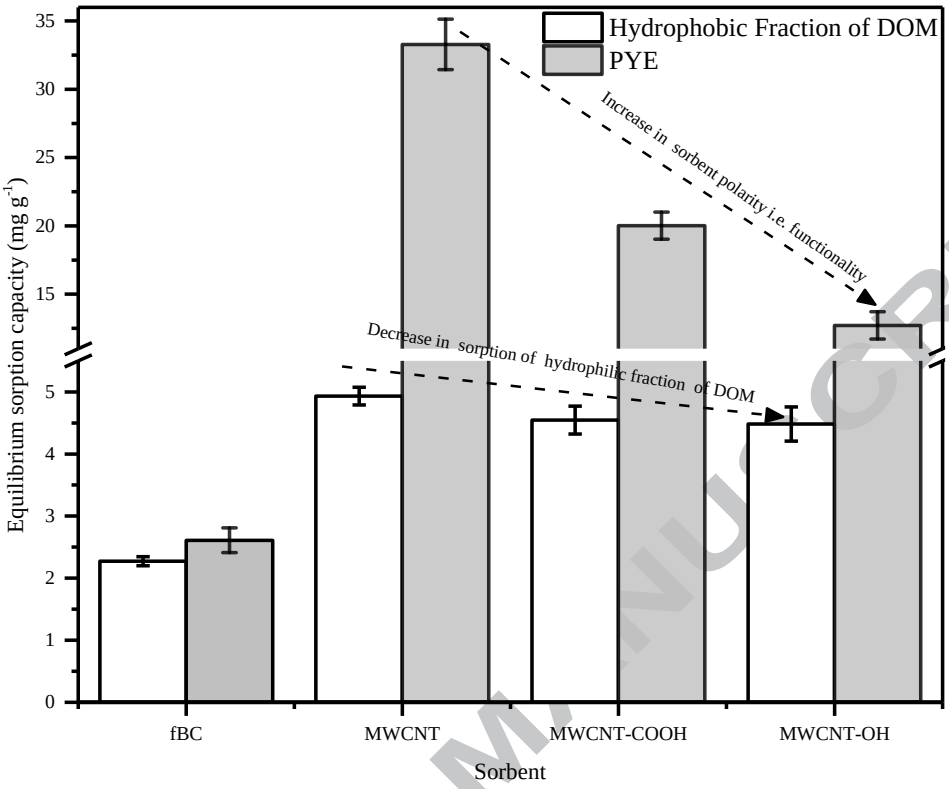

Figure 3

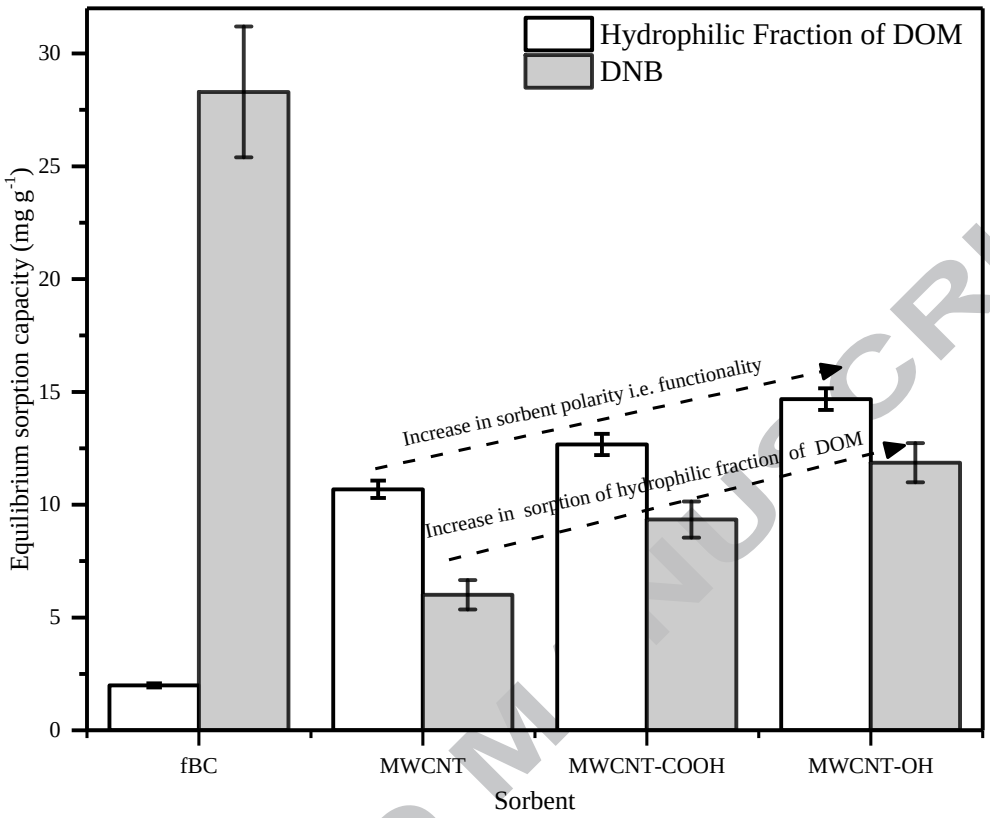

Figure 4

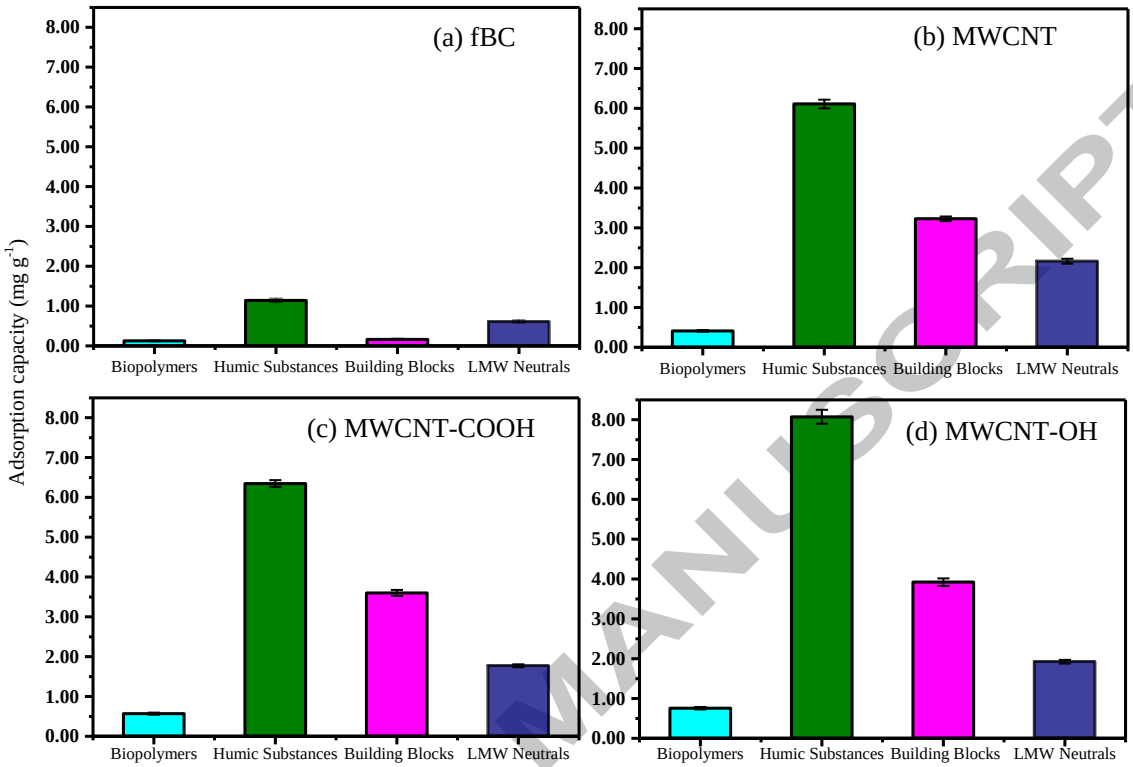

Figure 5

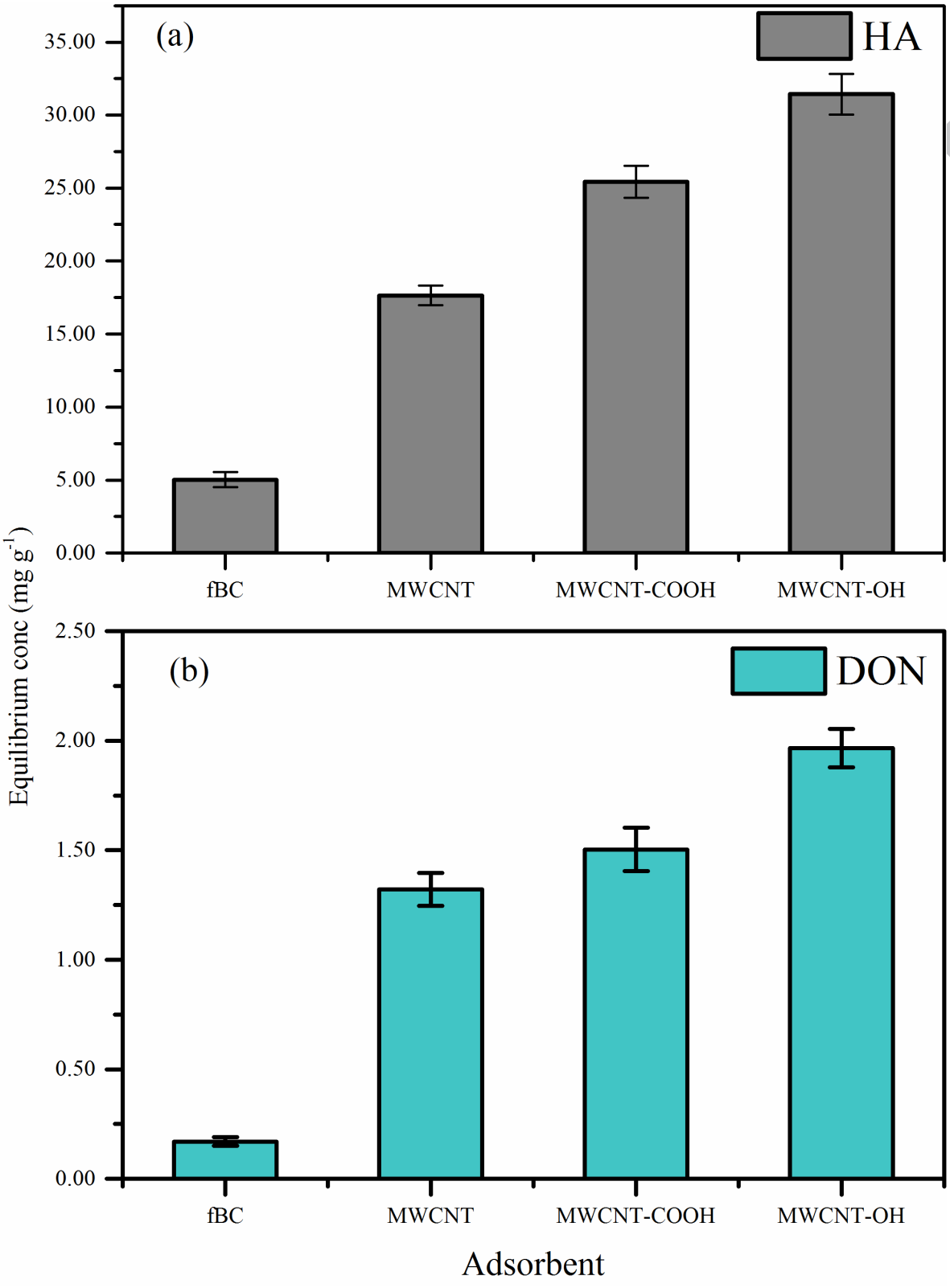

Table 1

Physicochemical characteristics of MBR sewage effluent.

Parameter	Value
pH	7.94±0.06
Conductivity (μS cm^{-1})	795±5
Dissolved organic matter, DOM (mg L^{-1})	8.63
Inorganic carbon (mg L^{-1})	48.15
Turbidity (NTU)	0.42
UV_{254} (cm^{-1})	0.269±0.02
Alkalinity (mg $CaCO_3$ L^{-1})	29.5
Chemical oxygen demand, COD (mg L^{-1})	28.3
Dissolved oxygen, DO (mg L^{-1})	5.39
Cl^- (mg L^{-1})	20.56
Br^- (mg L^{-1})	0.067
NO_3^- (mg L^{-1})	35.97
NO_2^- (mg L^{-1})	0.637
PO_4^{3-} (as P) (mg L^{-1})	12.67
SO_4^{2-} (mg L^{-1})	33.02
Na^+ (mg L^{-1})	198.96
K^+ (mg L^{-1})	31.42
Ca^{2+} (mg L^{-1})	12.90
Mg^{2+} (mg L^{-1})	4.72
Fe^{3+} (mg L^{-1})	0.10
Al^{3+} (mg L^{-1})	0.49

Table 2

UV_{254} values and SUVA values after adsorption with different CMs. Initial MBR effluent UV_{254} value and SUVA were 0.269 and 3.26, respectively.

Material	UV_{254} (cm^{-1})	SUVA (L mg^{-1} m^{-1})
fBC	0.203	2.99
MWCNT	0.138	2.35
MWCNT-COOH	0.132	2.15
MWCNT-OH	0.138	2.22

Table 3

Summary of the Langmuir and Freundlich isotherm parameters for DOM adsorption at 25±0.5 ^{0}C.

	Langmuir Isotherm				Freundlich Isotherm			
Sorbent	q_{max} (μg g^{-1})	K_L	r^2	$Adjr^2$	K_F	n	r^2	$Adjr^2$
fBC	7.81±0.61	0.151±0.02	0.997	0.994	1.32±0.002	0.58±0.001	0.996	0.996
MWCNT	39.29±6.13	0.098±0.02	0.996	0.992	4.11±0.005	0.71±0.006	0.998	0.998
MWCNT-COOH	36.23±6.55	0.140±0.04	0.990	0.981	5.32±0.008	0.64±0.001	0.997	0.997
MWCNT-OH	40.68±7.64	0.152±0.06	0.981	0.962	6.50±0.01	0.63±0.001	0.997	0.997

Table 4

Concentration of metal ions (ppm) in MBR effluents (pH 7.94±0.06) before and after sorption by different sorbents.

Material	Ca^{2+}	Mg^{2+}	Fe^{2+}	Al^{3+}	Cu^{2+}	Pb^{2+}	Ni^{2+}	Mn^{2+}
Before treatment	62.55	22.33	0.082	0.246	0.146	0.00164	0.0065	0.02314
fBC sorption	46.36	19.19	0.042	0.109	0.139	0.00108	0.0055	0.01175
MWCNT sorption	60.02	22.33	0.040	0.127	0.058	0.00141	0.0334	0.01985
MWCNT-COOH sorption	61.22	22.18	0.033	0.095	0.057	0.00073	0.0054	0.02156
MWCNT-OH sorption	57.61	21.81	0.082	0.148	0.090	0.00099	0.0047	0.02296

Highlights

- Sorption of DOM from MBR effluent by carbon materials was investigated.
- Sorbent functionality had great influence on sorption of DOM fractions.
- Hydrophobic fraction was better removed by MWCNT than functionalized sorbents.
- Hydrophilic fraction was better removed by functionalized MWCNTs than MWCNT.
- EDA, H-bond and hydrophobic interactions were the main sorption mechanism.